Hf-based high-k dielectrics for p-Ge MOS gate stacks

Sivan Fadida, Felix Palumbo, Laura Nyns, Dennis Lin, Sven Van Elshocht, Matty Caymax, and Moshe Eizenberg

Hf-based high-k dielectrics for p-Ge MOS gate stacks

Sivan Fadida[a)] and Felix Palumbo
Department of Materials Science and Engineering, Technion-Israel Institute of Technology, Haifa 3200003, Israel

Laura Nyns, Dennis Lin, Sven Van Elshocht, and Matty Caymax
Imec, Kapeldreef 75, B-3001 Leuven, Belgium

Moshe Eizenberg
Department of Materials Science and Engineering, Technion-Israel Institute of Technology, Haifa 3200003, Israel

The physical and electrical properties of the gate stack high-k/Al_2O_3/GeO_2/p-Ge were studied in detail, where the high-k is either HfO_2 or alloyed HfO_2 ($HfZrO_y$, $HfGdO_x$, or $HfAlO_x$). Electrical measurements combined with x-ray photoelectron spectroscopy chemical bonding analysis and band alignment determination were conducted in order to assess the suitability of hafnium-based high-k for this kind of gate stacks, with emphasis on low density of interface states and border traps. $HfAlO_x$ was found to be the most promising high-k from those studied. The authors have also found that the current- voltage trends for the various systems studied can be explained by the band alignment of the samples obtained by our x-ray photoelectron spectroscopy analysis. © *2014 American Vacuum Society*. [http://dx.doi.org/10.1116/1.4837295]

I. INTRODUCTION

Germanium is a leading candidate to serve as a future channel material of transistors due to its high carrier mobility (especially holes) with respect to Si.[1] Replacing Si channels with Ge leads to new challenges, stemming from lower interface quality and formation of unstable oxides. These properties of Ge require an effective passivation layer in order to achieve proper stability and electrical properties of the interface. Many attempts were done to optimize the passivation of the interface using several materials.[2–5] Passivation layers and carriers trapping at the Ge/oxide interface have become the core topic of Ge related researches.

GeO_2 used to be considered the cause for the low interface quality, and many attempts were made in order to avoid Ge oxidation. This was found to be very complicated. Moreover, very good passivation was achieved by growing a thin GeO_x (x < 2) layer as part of the passivation.[6,7] Since several routes for passivation of Ge were found, the current challenge in Ge MOS research is to find a gate dielectric with the desired properties. This dielectric should have a large band gap, large band offsets with respect to Ge, chemical and thermal stability on top of Ge or on top of the chosen passivation layer, and a high dielectric constant (high-k). Being at the center of attention as a high-k dielectric for Si MOSFET, HfO_2 is a natural candidate as a high-k dielectric for Ge gate stacks as well. Many attempts were made to alloy HfO_2 with another metal oxide in order to obtain a ternary oxide such as $Hf_xAl_{1-x}O_2$ (Refs. [8] and [9]) or $Hf_xGd_{1-x}O_2$ (Ref. [10]) with the goal of further improving its properties.[11] Some of the goals hoped to be achieved by alloying HfO_2 are increase of the dielectric constant, increase of the band gap and band offsets with respect to Ge,

reduction of oxygen vacancies, increase of the crystallization temperature, reduction of bulk and interface states, etc. It should be noted that usually in high-k dielectrics an increase in the dielectric constant is accompanied by a decrease in the band gap,[12] so not all goals can be achieved for a certain metal oxide. Unfortunately, HfO_2 was found to be unstable on GeO_2.[13,14] On the other hand, Al_2O_3 forms a very good interface with GeO_2 (Ref. [15]) but has a relatively low dielectric constant that hardly defines it as a high-k dielectric. Therefore, a multilayer gate stack of the structure: high-k/Al_2O_3/GeO_2/Ge where the high-k is HfO_2 or alloyed HfO_2 is considered in this study. This multilayer structure uses the best qualities of each layer- good interface qualities, high-k value, and adequate band alignment, as was shown to be effective in previous reports.[16–18] However, with such complex structures, the electrical characterization of the MOS capacitor is not straightforward and is affected by each of the layers and interfaces. For instance, density of interface traps (D_{it}) analysis using the conductance method can be difficult to interpret in such multilayer stacks since the loss in conductance cannot be attributed only to interface traps but also to oxide traps and border traps. We combine several electrical methods with chemical bonding characterization in order to determine which Ge MOS stack has the most promising properties. In this study, we are not necessarily focused in trying to obtain a minimal effective oxide thickness but in thoroughly understanding the chemical and physical properties of such structures, and the dependence of the electrical properties on those.

II. EXPERIMENT

A. Sample fabrication

The experiments were performed on 300 mm p-type Ge-on-Si wafers where 1 μm of undoped Ge was grown

---

[a)]Electronic mail: sivanfa@tx.technion.ac.il

epitaxially on top of the Si substrate. Afterwards, the wafers were cleaned for 30 s in a diluted HF solution (2 wt. %) to remove most of the native oxide. After the HF dip, the Ge surface was reoxidized in a controlled manner to obtain GeO_2 layers of ∼0.7 nm, as measured by x-ray photoelectron spectroscopy (XPS). Reoxidation was done during the atomic layer deposition (ALD) of ∼2 nm Al_2O_3 by means of the tri-methyl-aluminum (TMA)/O_3 process. GeO_x formation during this ALD process has been described before.[19,20] On top of the Al_2O_3/GeO_2 stack, ∼4 nm of an Hf-based high-k was deposited. These high-k layers consisted of HfO_2, $HfAlO_x$, $HfGdO_x$, or $HfZrO_y$ and were all deposited by ALD. The Hf:M atomic ratio was 1:1. The ALD was performed at 300 °C in a cross-flow ASM Pulsar 3000 reactor, attached to a Polygon8300 platform. The precursors used in the ALD process were: $HfCl_4$ and H_2O for HfO_2 deposition, TMA and Gd(iPrCp)$_3$ combined with $HfCl_4$ and H_2O for $HfAlO_x$ and $HfGdO_x$ deposition, respectively. Only $HfZrO_y$ was deposited at 250 °C in a top-flow ALD reactor of Applied Materials using tetrakis diethyl amino-hafnium, tetrakis diethyl amino-zirconium, and H_2O. A reference sample with the structure ∼4 nm Al_2O_3/GeO_2 was also fabricated on Ge. Pt was used as the gate electrode. All samples underwent a postdeposition anneal for 30 min at 400 °C in a gas-flow furnace using a forming gas 90%N_2+10%H_2 ambient. These annealing conditions were chosen after the results were compared with those of vacuum annealing (10^{-7} Torr, 30 min in 400 °C) and found to be significantly better.

B. Characterization

XPS measurements were conducted in a Thermo VG Scientific Sigma Probe system using a monochromatic Al Ka (1486.6 eV) x-ray source. Curve fitting was done by the XPSPEAK4.1 fitting program using a Gaussian–Lorentzian convolution (15%) with a Shirley-type background. Different XPS measurements induce different charging levels of the insulator sample. Charging compensation in all samples was done by aligning the Al 2p peak. This charge removal method can be somewhat problematic when dealing with the $HfAlO_x$ sample, since Al can also be found in the $HfAlO_x$ layer. In order to assure the charge removal procedure, two additional etched samples were prepared for the HfO_2 and $HfAlO_x$ samples. The top layer was gradually etched (1:10 HF and 1:20 HF, respectively) in order to enable the observation of the Ge 3d peak from the substrate, along with the Hf 4f and Al 2p peaks. In this way, it was possible to remove the charging effect using the Ge 3d (29.4 eV) transition. The reference sample was used in order to determine the band edges of Ge and Al_2O_3. Cross sectional transmission electron microscopy (TEM) samples were prepared by conventional polishing and were examined in a 200 keV FEI Tecnai G2 T20 Twin TEM.

All electrical measurements were performed at room temperature in a probe station sealed from light. Steady state capacitance voltage (C-V) measurements were conducted using an HP4284 LCR meter at various frequencies (10 kHz–1 MHz). Current voltage (I-V) measurements were

conducted using an Agilent 4155C parameter analyzer under a negative bias in order to test the leakage current behavior in accumulation conditions.

III. RESULTS AND DISCUSSION

TEM micrographs presented in Fig. 1 show uniform layers. No crystallinity or phase separations in the high-k ternary or binary oxides are observed. Also, for none of the samples the thin GeO_2 layer is observed. This is probably due to similar contrasts caused by similar molecular weights of Al_2O_3 and GeO_2. In order to verify that indeed there is a layer of oxidized Ge, we have examined the Ge 3d peak of the etched samples. The spectrum is taken from a region where there is still a signal from the top high-k layer meaning the layer was not completely etched. This examination confirms that oxidized Ge is present in the samples (Fig. 2). Two oxidation states of Ge are identified: Ge^{4+} and Ge^{2+}, where the compounds ratio calculated from the peaks areas is 20:3. From this ratio, we can surely state that the type of the oxide is mostly GeO_2 since the dominant oxidized Ge peak corresponds to the oxidation state of Ge^{4+}. Al bonding to oxidized Ge at the Al_2O_3/GeO_2 interface can also contribute to the oxidized Ge peak, but probably in a smaller amount.

C-V Measurements of various frequencies were conducted on the samples. It is clearly seen from the C-V measurements (Fig. 3) that each of the elements added to HfO_2 improves the C-V characteristics as will be discussed below. This observation is consistent for all frequencies measured. C-V curves at low frequencies [Fig. 3(a)] show, as expected, the weak inversion hump behavior. When comparing the weak inversion hump area for all samples [inset of Fig. 3(a)], we see a clear difference between the samples. Since
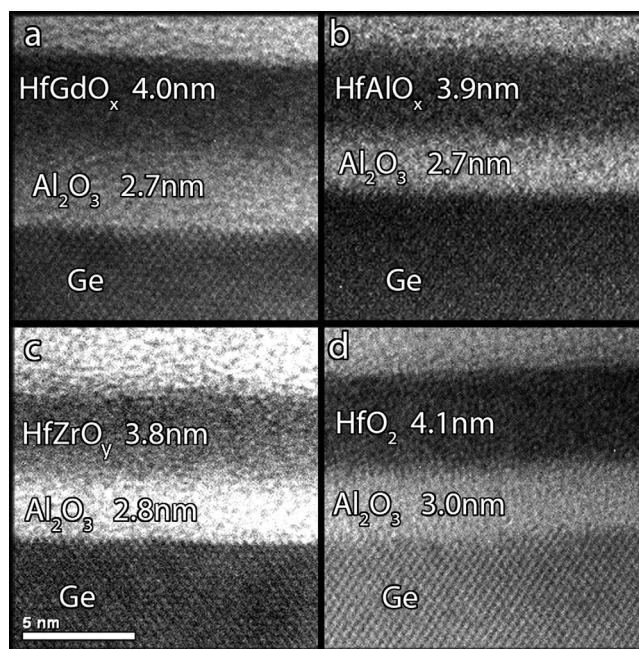

FIG. 1. Cross section TEM micrographs of (a) HfGdOx, (b) HfAlOx, (c) HfZrOy, and (d) HfO2. All images show uniform high-k layers with quite abrupt interfaces.
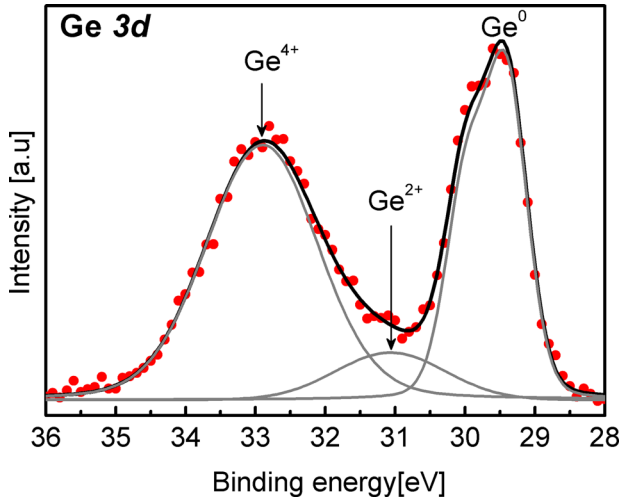
FIG. 2. (Color online) Ge 3d spectra (background subtracted) taken from the HfAlO$_x$ sample after a graded etch procedure. The spectrum is taken from a region where there is still a signal from the top high-k layer meaning the layer was not completely etched. This spectrum shows the major oxidized Ge component is Ge^{4+} corresponding to GeO$_2$.

this hump area is proportional to the amount of mid-gap states,[21] we conclude that the reduction of these states is significant in all HfMO$_x$ samples when compared to the HfO$_2$ sample. The smallest weak inversion hump area is of the HfZrO$_y$ sample.
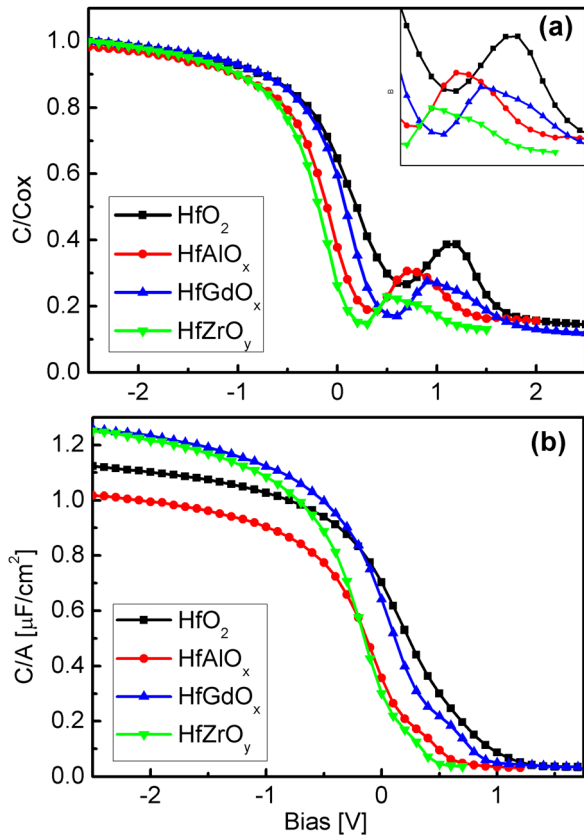

FIG. 3. (Color online) C-V curves of all samples at (a) 10 kHz and at (b) 100 kHz. Inset of Fig. 3(a) shows a magnification of the weak inversion region showing a clear difference between samples, although all have the same passivation structure. Figure 3(b) shows the difference of the relative permittivity value.

Figure 3(b) demonstrates the differences between the Hf-based high-k dielectrics in terms of the dielectric constant. Using the accumulation capacitance values and the total thickness of the dielectric stack measured by TEM, we have calculated the effective dielectric constant of the HfMO$_x$/Al$_2$O$_3$/GeO$_2$ dielectric stack for our samples. The effective dielectric constant was found to be 8.5, 7.7, 9.5, and 9.5 for M being Hf, Al, Gd, and Zr, respectively. Those values are lower than what we would have expected for Al$_2$O$_3$/HfMO$_x$ bilayers. The lowering of the effective k is probably due to the GeO$_2$ layer. We can conclude that adding Zr or Gd to HfO$_2$ increases the effective permittivity, while Al addition decreases it. This conclusion is drawn since the difference between the samples is in the top layer only.

The D$_{it}$ analysis (Fig. 4), preformed by the conductance method,[22] indicates a large trap density around midgap repeatedly for all samples. When the hump area is compared to the D$_{it}$ value, a good correlation is observed for HfO$_2$, HfAlO$_x$, and HfZrO$_y$ but not for the HfGdO$_x$ sample. The traditional conductance method uses the assumption that the loss in the measured conductance is only caused by D$_{it}$. This assumption is reasonable for SiO$_2$/Si stacks, but may not be valid for the complex multi-layer stacks studied here, or for the majority of alternative channel materials for MOS capacitors.[22] Therefore, for instance, the C-V of the HfGdO$_x$ sample does not show such a good correlation with the D$_{it}$ analysis.

In order to understand the root cause of this inconsistency, we used the quasistatic C-V method[23] for a qualitative evaluation of interface traps as well as border traps (Fig. 5). This method enables to separate between the contributions of each kind of traps, a separation which is not possible in the conductance method. Border traps cause broadening of the quasistatic C-V curve, while interface traps increase its minimum capacitance.[20] The minimum capacitance of the HfGdO$_x$ sample curve implies a relatively low D$_{it}$, which fits the low hump area shown in Fig. 3(a). On the other hand, the relative high width of the HfGdO$_x$ quasistatic C-V curve implies a high border traps concentration, which can explain
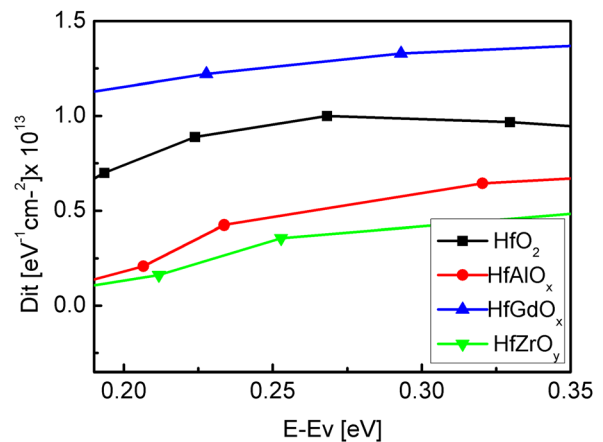

FIG. 4. (Color online) D$_{it}$ calculated for all samples using the conductance method. Here again a clear difference in the D$_{it}$ characterization is observed when the HfGdO$_x$ sample stands out with the highest D$_{it}$ among all samples studied.
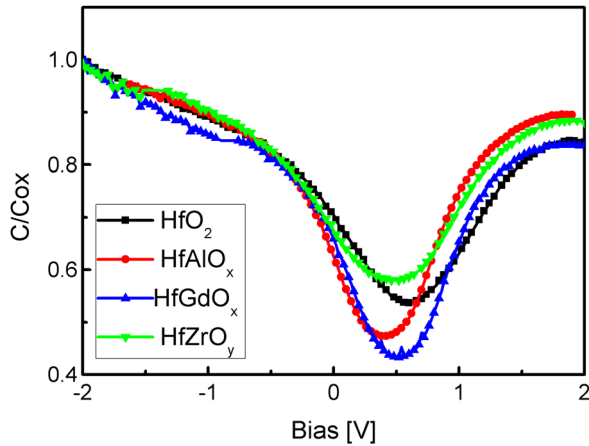
FIG. 5. (Color online) Quasistatic C-V curves of all samples. Here the $HfZrO_y$ sample shows the highest D_{it} (shallowest curve) and the $HfGdO_x$ sample (together with the HfO_2 sample) shows the highest density of border traps (widest curve).

the high conductance loss measured for this sample. Therefore, we conclude that this conductance loss is due to border traps rather than interface traps. Here it is again clear that the HfO_2 sample has the worst properties in terms of trap densities in comparison to the studied ternary $HfMO_x$ samples (M = Al, Gd, Zr). Based on the quasistatic C-V and the D_{it} analysis, it appears that the $HfAlO_x$ sample has the best properties when considering interface and border traps.

This conclusion is further validated when we analyze the oxygen bonding by XPS (Fig. 6). The O1s spectra collected from the samples are relatively similar. High similarity is observed for the O1s spectra of HfO_2 and $HfZrO_y$ due to a significant chemical similarity between Zr and Hf. Each of the four spectra presented in Fig. 6(a) consists of one major peak at a binding energy of ~530 eV corresponding to the Hf-O bonding. The same binding energy and full width at half maximum are observed in the Hf-O peak of all the samples. This implies that the Hf-O bonding does not change drastically when another metal atom is added to HfO_2. The second component of the O1s spectrum is at a binding energy of ~531 eV corresponding to the Al-O bonding from the underlying Al_2O_3. The intensity of this peak is relatively smaller than the Hf-O peak, but is larger for the $HfAlO_x$ sample since the Al-O bonding exists in the top high-k layer in addition to its contribution from the underlying Al_2O_3. Another small component that exists for all samples is at a binding energy of ~532.5 eV corresponding to C-O bonding from surface contamination. In the O1s spectrum of the $HfGdO_x$ sample, we can clearly see another component that is not observed in the other samples. The detailed peak fitting of the O1s spectrum for this sample is presented in Fig. 6(b). The additional component at binding energy of ~531.7 eV is attributed to O-H bonding due to water adsorption. Gd oxide, as well as other rare earth oxides, is known for its hygroscopic nature.[24] We assume that this leads to the observed high defect density and also border traps.

Another indication for the high-k stack quality is the C-V hysteresis measurement (Fig. 7). The measurement was done
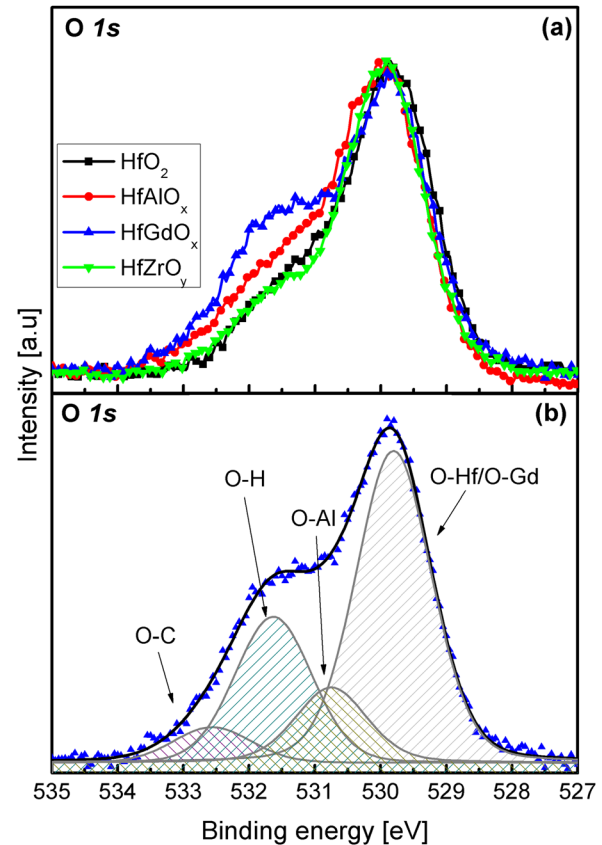

FIG. 6. (Color online) (a) O1s spectra (background subtracted) taken from all samples. The figure shows the data points as collected without peak fitting. (b) O1s spectrum (background subtracted) taken from the $HfGdO_x$ sample. Peak fitting reveals four different types of oxygen bonding (marked), including O-H bonding attributed to water adsorption.

in a retrace mode where the voltage was swept from inversion to accumulation and back to inversion. Here, in contrast to the other electrical characterizations done, there is no big difference between the HfO_2 and the $HfGdO_x$ and $HfZrO_y$ samples, and all show a large hysteresis (0.6 V, 0.7 V, and 0.6 V, respectively), indicating a large density of charged
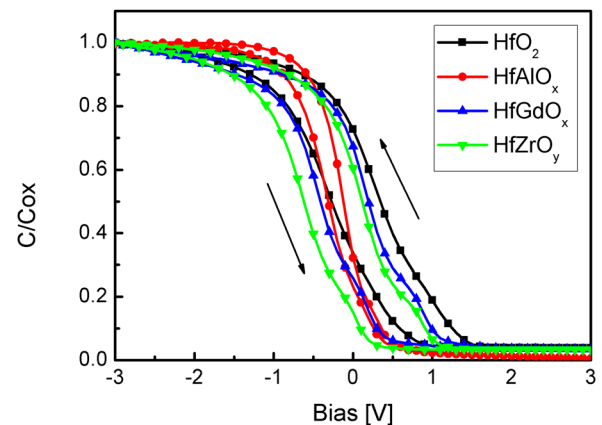

FIG. 7. (Color online) Hysteresis C-V curves at 100 kHz. The width of the hysteresis loop is 0.6–0.7 V for the $HfO_2 HfZrO_x$ and $HfGdO_x$ samples, while it is only 0.2 V for the $HfAlO_x$ sample.

defects, namely border traps.[25,26] The border traps density (N_{bt}) was estimated using

$$N_{bt} = \frac{\Delta V \cdot C_{ox}}{q}, \qquad (1)$$

where ΔV is the hysteresis in V, C_{ox} is the oxide capacitance in F/cm^2, and q is the elementary charge in C. The N_{bt} values are $4.2 \cdot 10^{12}$, $4.7 \cdot 10^{12}$, $5.5 \cdot 10^{12}$ (cm^{-2}) for HfO$_2$, HfGdO$_x$, and HfZrO$_y$, respectively.

On the other hand, it is clear that the HfAlO$_x$ sample is with the smallest hysteresis measured (0.2 V) and N_{bt} of 7.25×10^{11} (cm^{-2}). This corresponds well with the previous results and is another validation of the relatively low concentration of border traps in the HfAlO$_x$ sample.

Current–voltage (I-V) measurements were also conducted. The curves (Fig. 8) are presented as a function of the electric field, E (V/cm). The results show a significant difference between HfAlO$_x$ and the other high-k studied. While HfO$_2$, HfGdO$_x$, and HfZrO$_y$ display similar I-V curves, with the same trend and the same level of leakage current, the leakage current of the HfAlO$_x$ containing sample is one order of magnitude lower in the high field regime. In the low field regime, the leakage current of the HfAlO$_x$ sample seems slightly higher than for the other samples. Since it is very close to the sensitivity limit of the equipment, we believe it can be considered as noise fluctuation.

In order to understand the root cause of this phenomenon, the band alignments of the samples were determined using XPS further to our previous work on the Hf-Zr oxide system.[27] In this method,[28,29] the valence band offset (VBO) from the band edge of the substrate is measured by the XPS low energy spectrum, and the band gap is measured using the O1s energy loss spectrum. Then, the conduction band offset (CBO) is calculated by

$$CBO = Eg_{oxide} - Eg_{Ge} - VBO, \qquad (2)$$

where Eg_{oxide} and Eg_{Ge} are the oxide and Ge band gaps, respectively. We have used a reference sample (Al$_2$O$_3$/GeO$_2$/Ge) for the determination of the Al$_2$O$_3$ band

FIG. 9. (Color online) Valence band spectra for the HfO$_2$ HfAlO$_x$ and the reference sample. The first onset for the reference sample spectrum (empty squares) represents electrons ejected from the Ge valence band. The onset marked on the HfO$_2$ spectrum represents the electrons ejected from the HfO$_2$ valence band. The difference between them is the VBO of HfO$_2$ relative to Ge. The same holds for the HfAlO$_x$ spectrum.

gap and VBO with respect to Ge. The band gaps of Al$_2$O$_3$ (6.9 eV) and HfO$_2$ (5.4 eV) fit previous reports of amorphous ALD thin layers.[30,31] The VBO of the Hf based samples was measured with respect to the reference sample (Fig. 9). The band alignment is presented in Fig. 10. Here, again, the HfAlO$_x$ sample stands out: only in this high-k dielectric the VBO with respect to Ge is larger than the VBO of Al$_2$O$_3$ (3.6 and 3.1 eV, respectively), while for the other dielectrics, it is equal to the VBO of Al$_2$O$_3$ or smaller (3.0–3.1 eV). Examination of the CBO shows no difference between the samples. The CBO of the Hf-based high-k dielectrics with respect to Ge are in the range of 1.5–1.7 eV, all significantly smaller than the CBO of Al$_2$O$_3$ with respect to Ge (3.1 eV).

The band alignment shows that the HfAlO$_x$ sample has a significantly larger and thicker barrier for hole tunneling from the valence band as illustrated in Fig. 11. It also shows that the barrier for electron tunneling from the conduction band is the same for all samples and is dominated by the Al$_2$O$_3$ large CBO. From these observations, we suggest that the reduction in the leakage current of the HfAlOx sample (Fig. 8) can be explained by the reduction of hole tunneling current through the high-k dielectric. The dominant
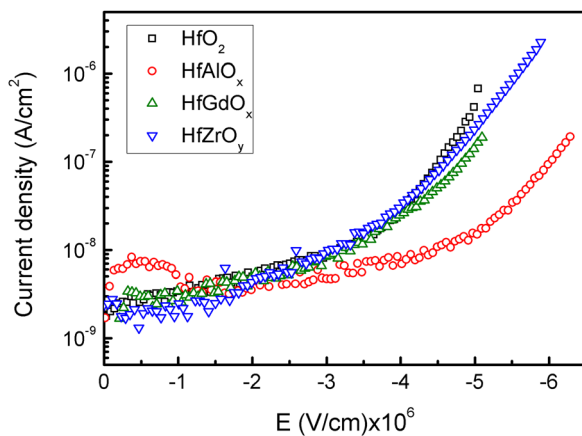

FIG. 8. (Color online) J-E curves for all samples showing a significant difference in the leakage current of HfAlOx sample under high electric fields.
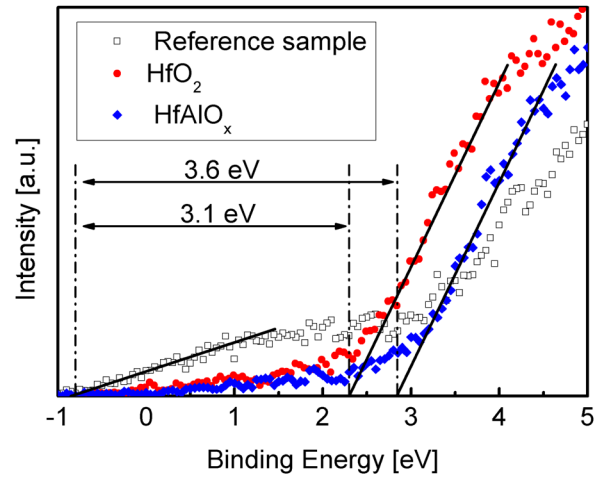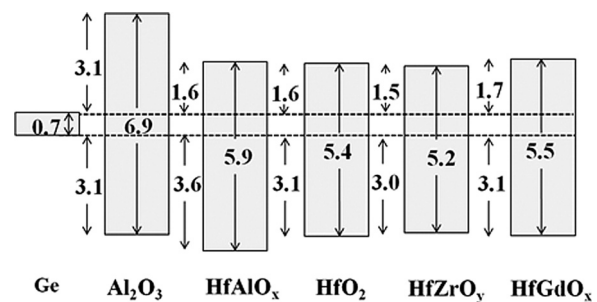

FIG. 10. Band alignment for all samples studied was determined using XPS. All values marked are given in eV. HfAlO$_x$ shows the largest VBO with respect to Ge while no significant difference is observed in the CBO.
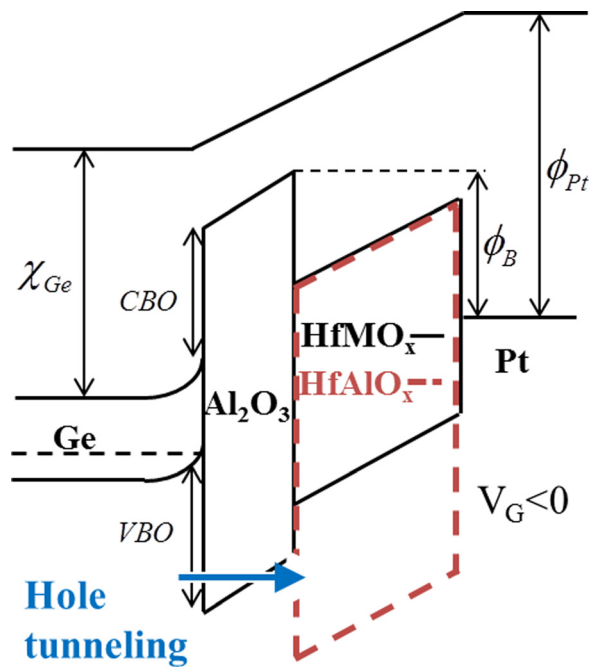
FIG. 11. (Color online) Schematic band diagram for the p-Ge MOS structures studied. The dashed red line represents the HfAlOx sample which has a larger VBO than the one of Al$_2$O$_3$. The hole tunneling is illustrated with the blue arrow.

mechanism of transport in the studied stacks cannot be determined without conducting further experiments. Beside the energy barrier for tunneling, we must consider that the effective mass of the holes in HfO$_2$ can change when another element is added to HfO$_2$. However, a change in the energy barrier has a larger impact on the tunneling current than a change in the effective mass.[32]

In order to establish this conclusion, we have also measured the leakage current of the reference sample with the structure Al$_2$O$_3$/GeO$_2$/Ge. The results are shown in Fig. 12 along with the J-V curves of the HfO$_2$ sample and of the HfAlO$_x$ sample for comparison. The leakage current of the reference sample is indeed higher than that of the HfAlO$_x$ sample, as can be expected based on the different VBO of Al$_2$O$_3$ and HfAlO$_x$. However, the leakage is still lower than
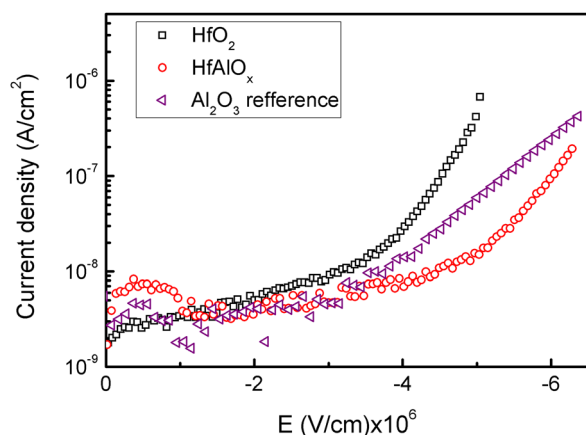

FIG. 12. (Color online) J-E curves for HfO$_2$, HfAlO$_x$, and the reference sample.

that of the HfO$_2$ sample. One possible explanation to the reduced leakage current in the reference sample is relying on the assumption that more than one tunneling mechanism is active and as an example the tunneling of electrons in the opposite direction to that of holes cannot be neglected. The barrier for electron tunneling ϕ_B as illustrated in Fig. 11 is determined by

$$\phi_B = \phi_{Pt} - (\chi_{Ge} - CBO_{Al_2O_3}), \qquad (3)$$

where χ_{Ge} is Ge electron affinity (4.0 eV), and ϕ_{Pt} is the Pt work function (5.65 eV).[33] For all samples ϕ_B is determined by Al$_2$O$_3$ CBO (3.1 eV) since this is the largest CBO in each sample studied. It is calculated to be 4.75 eV. For the reference sample this barrier is continuous for a distance of 4 nm (Al$_2$O$_3$ thickness in the reference sample) as opposed to only 2 nm in the Hf-based samples. This can reduce the current contributed by electron tunneling in the reference sample. The results of the I-V measurements further establish that for all high-k studied in this work HfAlO$_x$ is the most appropriate one.

IV. CONCLUSIONS

In this paper, we have thoroughly studied the high-k/Al$_2$O$_3$/GeO$_2$/Ge p-MOS structure in order to find which Hf-based high-k has the most promising properties for a future high mobility channel gate stack. Electrical measurements, including C-V in different frequencies, conductance method measurements, quasi-static C-V, hysteresis C-V and I-V measurements were conducted and analyzed carefully. Oxygen bonding was analyzed from the XPS O1s spectrum. The analysis reveals that the O-H bonding exists only in HfGdO$_x$. This result is correlated with the high density of border traps measured in this sample. I-V measurements correlated to band alignment (determined by XPS) lead us to conclude that hole tunneling is the dominant current mechanism in the samples studied. We have found repeatedly that the ternary Hf-based high-k dielectrics show improvement of the electrical properties of HfO$_2$. HfAlO$_x$ presents the best results for all systems studied in terms of electrical properties. One possible explanation to this result, which is obtained from the majority of electrical characterizations, is that the Al in HfAlO$_x$ improves the quality of the HfMO$_x$/Al$_2$O$_3$ interface. Another possible reason for the superiority of HfAlO$_x$ can be a reduction of the oxygen vacancies in HfAlO$_x$: oxygen vacancies are known to be stable in HfO$_2$ and much less stable in Al$_2$O$_3$.[34] We also show that the addition of Al to HfO$_2$ results in a slight decrease in relative permittivity value. This trade-off between a significant improvement of the electrical properties and a small reduction in the k value is acceptable. Perhaps a smaller amount of Al added can maintain the electrical properties shown here with a smaller cost in reduction in k value.

[1]Y. Kamata, Mater. Today **11**, 30 (2008).

[2]C. Henkel, O. Bethge, S. Abermann, S. Puchner, H. Hutter, and E. Bertagnolli, Appl. Phys. Lett. **97**, 152904 (2010).

[3]P. McIntyre *et al*., ECS Trans. **3**, 519 (2006).

[4]P. W. Loscutoff and S. F. Bent, Ann. Rev. Phys. Chem. **57**, 467 (2006).

[5]S. Sioncke *et al*., J. Appl. Phys. **110**, 084907 (2011).

[6]A. Delabie, F. Bellenger, M. Houssa, T. Conard, S. V. Elshocht, M. Caymax, M. Heyns, and M. Meuris, Appl. Phys. Lett. **91**, 082904 (2007).

[7]S. Takagi, R. Zhang, and M. Takenaka, Microelectron. Eng. **109**, 389 (2013).

[8]R. Suri, C. J. Kirkpatrick, D. J. Lichtenwalner, and V. Misra, Appl. Phys. Lett. **96**, 042903 (2010).

[9]X. F. Li, X. J. Liu, W. Q. Zhang, Y. Y. Fu, A. D. Li, H. Li, and D. Wu, Appl. Phys. Lett. **98**, 162903 (2011).

[10]Y. Xiong, H. Tu, J. Du, M. Ji, X. Zhang, and L. Wang, Appl. Phys. Lett. **97**, 012901 (2010).

[11]J. H. Choi, Y. Mao, and J. P. Chang, Mater. Sci. Eng. Rep. **72**, 97 (2011).

[12]J. Robertson, J. Vac. Sci. Technol. B **18**, 1785 (2000).

[13]O. Renault, L. Fourdrinier, E. Martinez, L. Clavelier, C. Leroyer, N. Barret, and C. Crotti, Appl. Phys. Lett. **90**, 052112 (2007).

[14]E. Golias, L. Tsetseris, A. Chroneos, and A. Dimoulas, Microelectron. Eng. **104**, 37 (2013).

[15]S. Swaminathan, Y. Sun, P. Pianetta, and P. C. McIntyre, J. Appl. Phys. **110**, 094105 (2011).

[16]J. Ahn, I. Geppert, M. Gunji, M. Holland, I. Thayne, M. Eizenberg, and P. C. McIntyre, Appl. Phys. Lett. **99**, 232902 (2011).

[17]H. X. Xu, J. P. Xu, C. X. Li, and P. T. Lai, Appl. Phys. Lett. **97**, 022903 (2010).

[18]S. Swaminathan, M. Shandalov, Y. Oshima, and P. C. McIntyre, Appl. Phys. Lett. **96**, 082904 (2010).

[19]A. Delabie *et al*., ECS Trans. **16**, 671 (2008).

[20]L. Nyns, D. Lin, G. Brammertz, F. Bellenger, X. Shi, S. Sioncke, S. V. Elshocht, and M. Caymax, ECS Trans. **35**, 465 (2011).

[21]I. Krylov, L. Kornblum, A. Gavrilov, D. Ritter, and M. Eizenberg, Appl. Phys. Lett. **100**, 173508 (2012).

[22]E. H. Nicollian and J. R. Brews, *MOS (Metal Oxide Semiconductor) Physics and Technology* (Wiley, New York, 1982).

[23]R. Engel-Herbert, Y. Hwang, and S. Stemmer, J. Appl. Phys. **108**, 124101 (2010).

[24]K. Wandelt and C. R. Brundle, Surf. Sci. **157**, 162 (1985).

[25]D. M. Fleetwood, IEEE Trans. Nucl. Sci. **39**, 269 (1992).

[26]D. M. Fleetwood, M. R. Shaneyfelt, W. L. Warren, J. R. Schwank, T. L. Meisenheimer, and P. S. Winokur, Microelectron. Reliab. **35**, 403 (1995).

[27]S. Fadida, M. Eizenberg, L. Nyns, S. Van Elshocht, and M. Caymax, Microelectron. Eng. **88**, 1557 (2011).

[28]S. Miyazaki, Appl. Surf. Sci. **190**, 66 (2002).

[29]I. Geppert, E. Lipp, R. Brener, S. Hung, and M. Eizenberg, J. Appl. Phys. **107**, 053701 (2010).

[30]E. Bersch, S. Rangan, R. A. Bartynski, E. Garfunkel, and E. Vescovo, Phys. Rev. B **78**, 085114 (2008).

[31]K. Y. Gao, T. Seyller, L. Ley, F. Ciobanu, G. Pensl, A. Tadich, J. D. Riley, and R. G. C. Leckey, Appl. Phys. Lett. **83**, 1830 (2003).

[32]J.-P. Locquet, C. Marchiori, M. Sousa, J. Fompeyrine, and J. W. Seo, J. Appl. Phys. **100**, 051610 (2006).

[33]H. B. Michaelson, J. Appl. Phys. **48**, 4729 (1977).

[34]J. L. Gavartin, D. M. Ramo, A. L. Shluger, G. Bersuker, and B. H. Lee, Appl. Phys. Lett. **89**, 082908 (2006).